Table of Contents

1. INTRODUCTION....................7

1.1 Overview of Mir Photo/TV Survey....................7

1.2 Summary of Findings....................7
1.2.1 Mir Configuration....................8
1.2.2 Mir Surface Assessment....................8
1.2.3 Docking Mechanism Assessment....................8
1.2.4 Plume Impingement....................9
1.2.5 Motion Analysis from Film and Video....................9
1.2.6 Antenna Tracking....................9
1.2.7 Solar Array Sub-panel Deflection....................9
1.2.8 Imagery Evaluation....................9

2. MIR CONFIGURATION....................10

2.1 General Assessment....................10

2.2 Configuration Documentation Discrepancies....................16

3. MIR SURFACE ASSESSMENT....................18

3.1 Base Block....................18

3.2 Kvant Module....................21

3.3 Kristall Module Docking Mechanism....................23

3.4 Soyuz-TM Capsule....................25

3.5 Solar Arrays....................26

4. TARGET VIEWING ASSESSMENT....................29

4.1 Target Acquisition Times....................29

4.2 Target Visibility Comparison....................29

5. PLUME IMPINGEMENT....................31

5.1 Impingement Data....................31

5.2 Correlation with Shuttle RCS Thruster Firings....................31

6. MOTION ANALYSIS FROM FILM AND VIDEO....................32

Table of Contents

7. ANTENNA TRACKING..33

8. SOLAR ARRAY SUB-PANEL DEFLECTION..35

9. PRODUCT EVALUATION..36

9.1 Film Summary...36
9.1.1 35 mm Photography..37
9.1.2 70 mm Photography..37

9.2 Video Summary..37
9.2.1 Centerline (CTVC)..38
9.2.2 Payload Bay Camera 'A'...38
9.2.3 Payload Bay Camera 'B'...39
9.2.4 Payload Bay Camera 'C'...39
9.2.5 Payload Bay Camera 'D'...39
9.2.6 Camcorder..39

10. CONCLUSIONS AND RECOMMENDATIONS...41

10.1 Russian Review...41

10.2 Conclusions..41
10.2.1 Assessment of Procedures...41
10.2.2 Discussion of Results...41

10.3 Recommendations..42

10.4 Other Issues...42

11. APPENDICES..43

List of Figures

Figure 1-A	**Isometric View of STS-63 Configuration**	**8**
Figure 2-A	**Overview of Mir Complex**	**10**
Figure 2-B	**Progress M Capsule / Kvant 1 Module**	**11**
Figure 2-C	**Kvant 1 Module / Progress M / Mir Base Block**	**12**
Figure 2-D	**Mir Base Block / Kvant 1 Module / Kristall Module**	**13**
Figure 2-E	**Kristall Module / Mir Base Module**	**14**
Figure 2-F	**Kristall Docking Mechanism**	**15**
Figure 2-G	**Soyuz TM Capsule / Mir Module**	**16**
Figure 3-A	**Mir Base Block**	**19**
Figure 3-B	**Mir Base Block Working Compartment**	**20**
Figure 3-C	**Kvant Module**	**21**
Figure 3-D	**Kvant Module Forward Conical Section**	**22**
Figure 3-E	**Kristall Module APDU - Centerline**	**23**
Figure 3-F	**Kristall Module APDU - Off-center**	**24**
Figure 3-G	**Soyuz-TM Descent Module**	**25**
Figure 3-H	**Solar Array off Mir Base Block**	**26**
Figure 3-I	**Port Solar Array off Kristall Module**	**27**
Figure 3-J	**Starboard Solar Array off Kristall Module**	**28**
Figure 4-A	**Target Visibility Comparison**	**30**
Figure 6-A	**Shuttle/Mir Relative Distance During Approach and Backaway**	**32**
Figure 7-A	**Luch Antenna Arm Orientation**	**33**
Figure 7-B	**Luch Antenna Dish Orientation**	**34**
Figure 8-A	**Solar Array Sub-panel Nomenclature**	**35**

List of Tables

Table 4-A **Target Acquisition Times..29**

Table 8-A **Solar Array Offset Angles...35**

Table 9-A **Onboard Still Photography of Mir Rendezvous Events...................36**

Table 9-B **Onboard Video Coverage of Mir Rendezvous Events......................38**

1. INTRODUCTION

NASA and RSC-E are involved in a cooperative venture in which the Shuttle will rendezvous with the Mir Space Station during several missions over the next three years. This sequence of at least six missions will serve as a precursor to the two nations' involvement in the International Space Station. The rendezvous missions provide NASA scientists and engineers an excellent opportunity to study the orbital, dynamic, and environmental conditions of long duration spacecraft, as well as the opportunity to develop evaluation and risk mitigation techniques which have direct application to the International Space Station.

1.1 Overview of Mir Photo/TV Survey

Detailed Test Objective (DTO-1118) integrates the requirements for photographic and video imagery of the Mir Space Station generated by the engineering and science communities at the Johnson Space Center, including the Payload Integration and Engineering Office (MS2), the Space Science Branch (SN3), the Structures and Dynamics Branch (ES2), the Crew Station Branch (SP3), Guidance and Procedures (DM43), the Astronaut Office (CB) and the Space Station Program Office (OB).

The general objectives of the Mir Photo/TV Survey are as follows:

- Provide assurance of crew and orbiter safety while in the proximity of the Mir Station.
- Assess the overall condition of the Mir.
- Study the effects of the space environment on a long-duration orbiting platform.
- Understand the impact of plume impingement during proximity operations.
- Evaluate the equipment and procedures used to gather survey data.

STS-63 was the Shuttle's first rendezvous with the Mir station. Over 1000 photographs and 10 hours of video were acquired during the rendezvous. The Image Science & Analysis Group (IS & AG) initiated several analysis tasks using the returned imagery data based on user requirements. They were to:

- Verify the configuration of the Mir complex.
- Assess the effect of micro-meteoroid impacts on Mir surfaces.
- Document the condition of the docking mechanism.
- Analyze the effect of Shuttle RCS thruster firings on the Mir complex during approach and backaway.
- Determine the usefulness of imagery data in calculating approach and backaway velocities.
- Track the motion of a communications antenna on the Mir Base Block.
- Measure solar panel offset angles.
- Assess the quality of video and photographic data.

RSC-Energia has reviewed the contents of a preliminary version of this report and their remarks are included in Section 10.1.

1.2 Summary of Findings

A summary of findings from each of the aforementioned analysis tasks follows.

1.2.1 Mir Configuration

The isometric view shown in Figure 1-A labels the major station components. Both Guidance and Procedures (DM43) and the Structures and Dynamics Branch (ES2) are interested in verifying the configuration of the Mir station. This information could be important for proximity operations requiring visual navigation and for conducting loads simulations of docked configurations. Documentation of the Mir station was compared to photography acquired during the rendezvous. The most significant discrepancy found was that the Soyuz-TM and Progress capsules were at opposite ends of the Station from where they were expected.

Figure 1-A Isometric View of STS-63 Configuration

1.2.2 Mir Surface Assessment

The Space Science Branch (SN3) and the International Space Station Alpha Vehicle Architecture Integration Team are studying the effects of the space environment on materials used on the Mir station. Detailed photography of the surface of the Base Block revealed several possible micro-meteoroid impact locations. Other visible damage included a possible tear on the Soyuz capsule blanket used to protect against the effects of diurnal variance in temperature and apparent impacts on the Kristall and Base Block solar arrays. Also, several areas of discoloration were noted on the Mir Base Block.

1.2.3 Docking Mechanism Assessment

The Payload Integration and Engineering Office (MS2) is assessing the condition of the Kristall docking mechanism. STS-63 provided engineers with the last opportunity to evaluate the standoff docking target and other features on the docking mechanism prior to the STS-71 rendezvous. Both video footage and photographic data were acquired of the docking mechanism and target during the rendezvous. In general, the targets and surrounding area appeared to be free of damage and in good condition.

1.2.4 Plume Impingement

The Structures and Dynamics Branch (ES2) is concerned with the effects of plume impingement during the approach and backaway sequences. Anticipated data did not provide enough information for a quantitative analysis. However, video of the approach and backaway sequences revealed motion of a “foil” cover located on the Mir Base Block. Comparison of this motion with the Shuttle RCS thruster data revealed a direct correlation with the firing of the F2F and F3F thrusters.

1.2.5 Motion Analysis from Film and Video

The Image Science & Analysis Group (SN5) is evaluating the use of video and photographic data to measure motion. During approach and backaway procedures, the Trajectory Control System (TCS) was used to determine distances from the Orbiter to the Mir station. These numbers were compared to calculations made from photogrammetric analysis of both video and film data. This comparison will help future motion analyses when only imagery sources are available.

1.2.6 Antenna Tracking

The Payload Integration and Engineering Office (MS2) and Flight Planning and Pointing (DO45) are concerned with the changing orientation of the Luch antenna on the Mir Base Block. There may have been occurrences where the Mir antenna could be looking directly at the Shuttle Ku-band antenna. In the event of such an occurrence, damage to both communication systems could have resulted. Radiation resulting from antenna cone angles intersecting the Shuttle is also a crew safety issue. Estimates of Luch antenna pointing angles were generated.

1.2.7 Solar Array Sub-panel Deflection

The Structures and Dynamics Branch (ES2) is interested in unexpected offsets noted between sub-arrays on some Mir solar panels. Such deflections could have an impact on loads analysis when the Shuttle and Mir are in a docked configuration. While available imagery did not provide the best look-angles to determine these deflections, estimates were made on all such panels where measurements could be obtained.

1.2.8 Imagery Evaluation

The Image Science & Analysis Group (SN5) and the crew trainers from the Systems Division (DF43) are evaluating image data and acquisition procedures. Assessment of this data is being performed to identify problems with procedures and equipment for subsequent rendezvous missions. Recommendations have been made to change the primary still camera on STS-71 from the Nikon (35 mm) to the Hasselblad (70 mm), and to improve survey acquisition techniques.

2. MIR CONFIGURATION

2.1 General Assessment

A detailed assessment of the STS-63 configuration is presented. This involved identifying and labeling features directly from the photography. A comparison of expected and actual station elements revealed discrepancies between documentation and photography and these items are chronicled in section 2.2.

Documentation information was gathered from the sources listed below:

- Training Manual “A Russian Space Station: The Mir Complex”
- Manual “Soviet Space Stations as Analogs” - Vol. II, 3rd Edition
- JSC 26770 “Mir Hardware Heritage”
- Document WG-3/NPO-E/NASA/002/3402-0

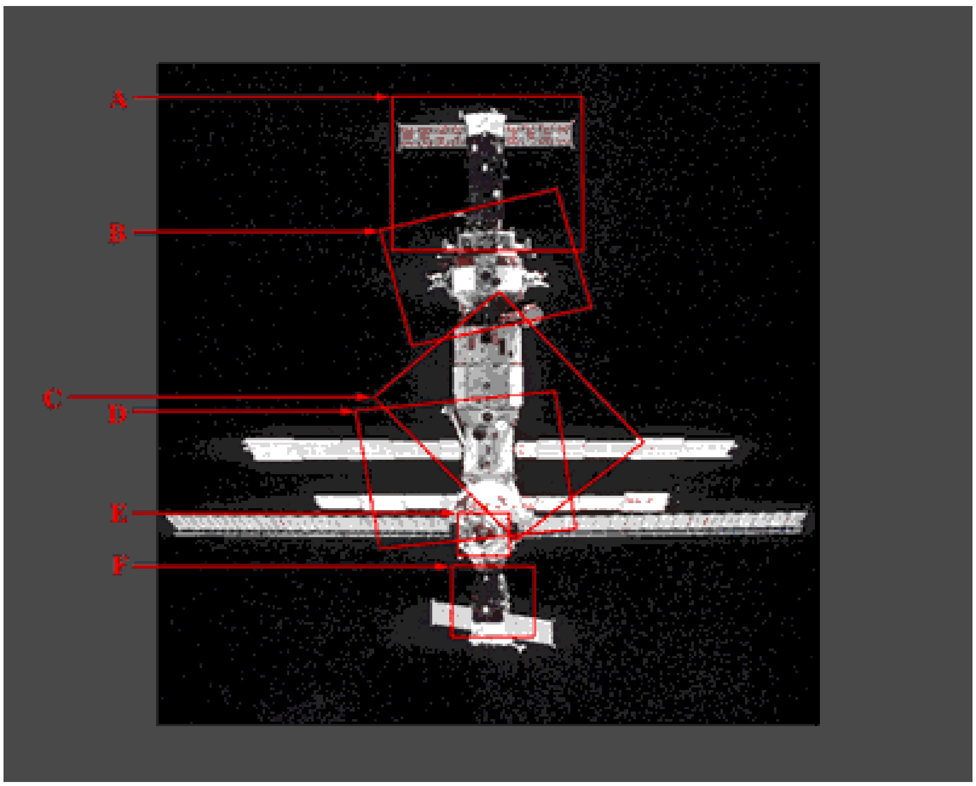

Figure 2-A Overview of Mir Complex

The boxes labeled A-F encompass regions whose exterior surfaces are described in detail within this section. Progress-M (Box A) is the unmanned logistics resupply spacecraft for Mir. Kvant-1 (Box B) is an astrophysics and attitude control module which was launched on March 31, 1987. The Mir Base Block (Boxes C, D) was launched in February of 1986. Kristall (Boxes D, E) is a docking, materials processing, and Earth observation module which was launched on June 1, 1990. Soyuz TM (Box F) is used to transport cosmonauts between the Mir Complex and Earth. Kvant-2 (not seen because it is located opposite Kristall) augments Mir Base Block capabilities and provides an Extravehicular Activity (EVA) airlock. It was launched on November 26, 1989.

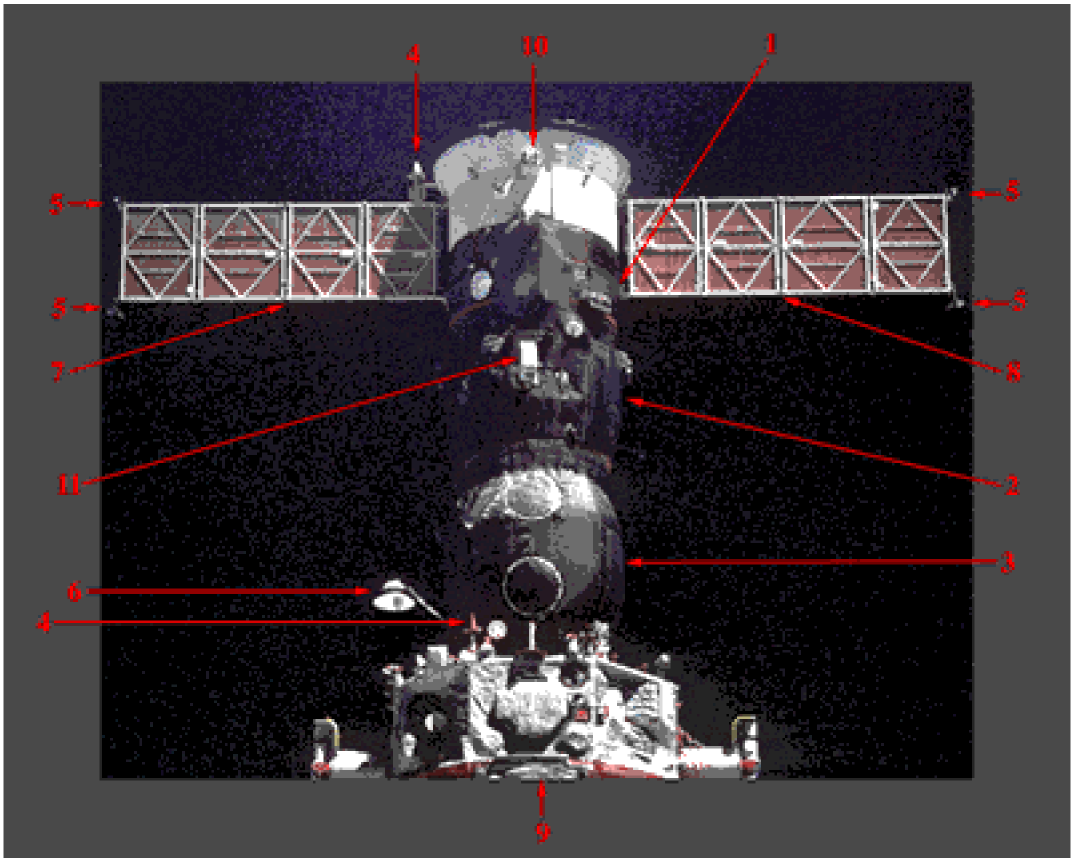

Figure 2-B Progress M Capsule / Kvant 1 Module

1. Instrument Section
2. Propellant Section
3. Cargo Section
4. Approach and Rendezvous (Igla) Antenna
5. Approach and Rendezvous (Igla) Antenna
6. Long Range Antenna
7. Left Solar Array
8. Right Solar Array
9. Kvant 1 Module
10. Horizon Sensor
11. Television camera covered by a protective housing with a white coating

A “white box” located in the middle of the propellant section is not labeled in any diagrams.

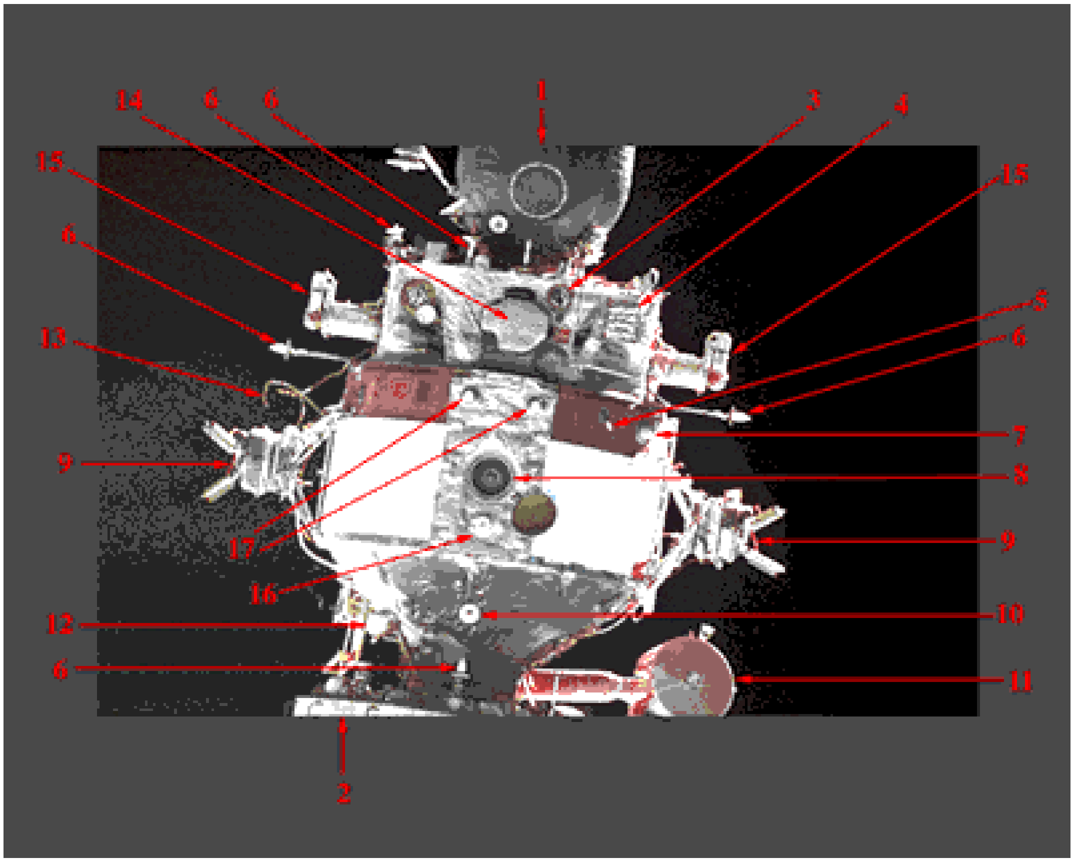

Figure 2-C Kvant 1 Module / Progress M / Mir Base Block

1. Progress M Capsule
2. Mir Base Block
3. "Siren" Spectrometer
4. Micrometeoroid Sensor
5. Radiotelemetry System Antenna
6. Approach and Rendezvous (Igla) Antenna
7. Infrared Sensor
8. Earth Observation Window
9. Solar Array Attach Port
10. Approach and Rendezvous (Igla) Antenna
11. Luch relay satellite Communications Antenna (11/14 Ghz)
12. "Kurs" Antenna
13. EVA Tethers
14. "Glazar" Telescope
15. Star sensor (to determine star coordinates)
16. Instrument for visual orientation on stars
17. Horizon Sensor with L-shaped overhangs

Two large "L" shape extensions on either side of Kvant 1 are not labeled in any diagrams.

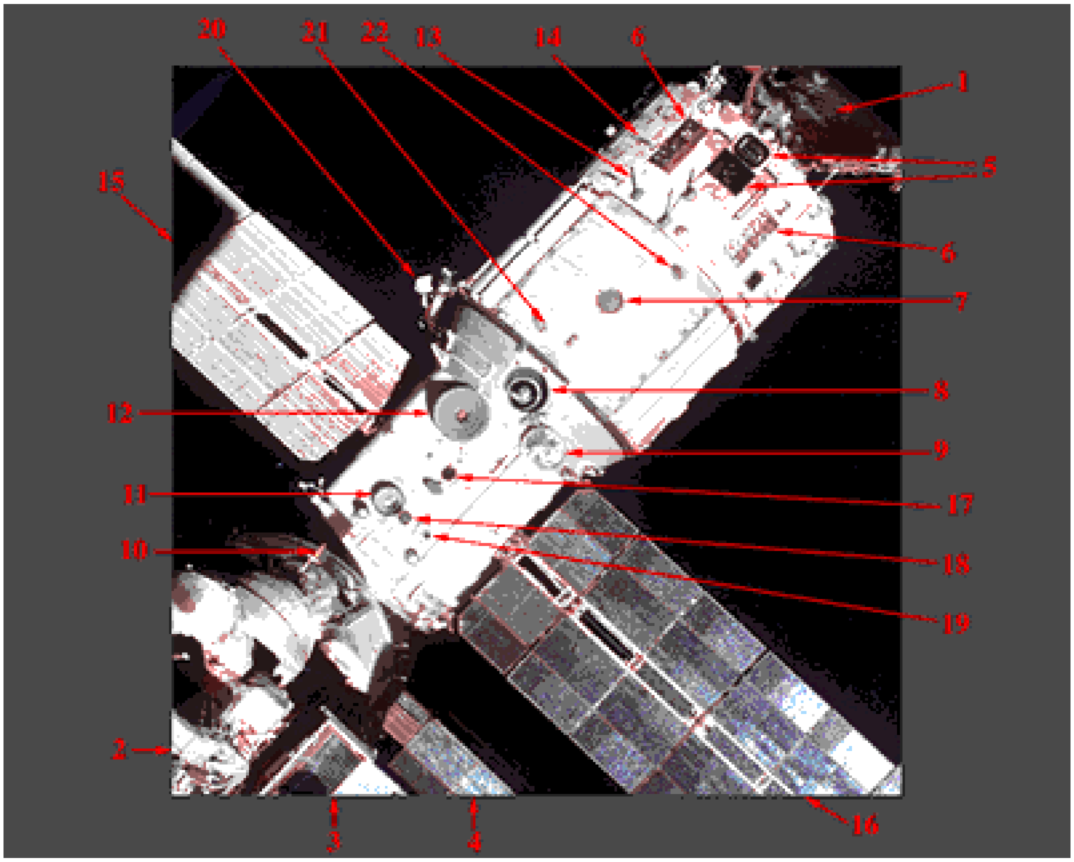

Figure 2-D Mir Base Block / Kvant 1 Module / Kristall Module

1. Kvant 1 Module
2. Kristall Module
3. Kristall Port Solar Array
4. Kvant 2 Starboard Solar Array (Kvant 2 is located below Kristall)
5. Attitude Control Thrusters
6. Micrometeoroid Sensor
7. Airlock Hatch Cover
8. Earth Observation Window
9. Window Cover With Flexible Metallic Surface
10. Approach and Rendezvous (Igla) Antenna
11. Window Blind
12. Observation Window Blind
13. Radio/Telemetry Communications Antennas
14. EVA Handrails
15. Mir Port Solar Array
16. Mir Starboard Array
17. Window with Cover
18. Cosmonaut’s Wide-angle Sight
19. Instrument for orientation on eclipsed orbital sections
20. Cargo Boom Base
21. Television Antenna
22. Flashing Light

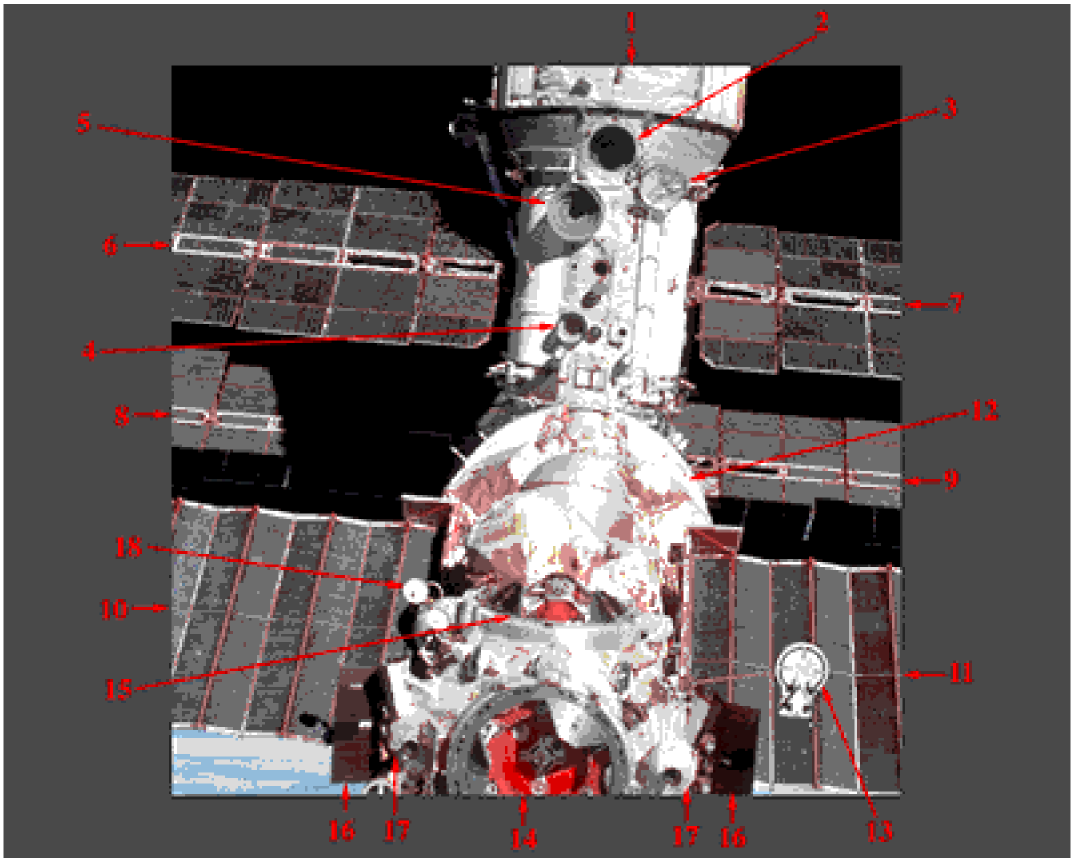

Figure 2-E Kristall Module / Mir Base Module

1. Mir Base Module
2. Earth Observation Window
3. Window Cover With Flexible Metallic Surface
4. Window Blind
5. Window Blind
6. Mir Port Solar Array
7. Mir Starboard Solar Array
8. Kvant 2 Port Solar Array
9. Kvant 2 Starboard Solar Array
10. Kristall Starboard Solar Array
11. Kristall Port Solar Array
12. Kristall Module
13. Kristall Target for Docking and Stationkeeping
14. Androgenous-Peripheral Docking Unit (APDU) 1
15. Androgenous-Peripheral Docking Unit (APDU) 2
16. Deflection Plates
17. Mooring and Stabilization Engines
18. “Kurs” Docking System Parabolic Antenna

The solar arrays of the Base block, Kvant 2, and Kristall are all visible in this image.

Figure 2-F Kristall Docking Mechanism

1. Sun Sensor
2. Fluid/Electrical Socket/Plug
3. Structural Latch (12)
4. Capture Latch (3)
5. Alignment Guides (3)
6. Body-mounted Latch (3)
7. Laser Retroreflector No. 3
8. Onboard Light (White)
9. Soyuz TM Target
10. Laser Retroreflector No. 2
11. Video Camera
12. Onboard Light (Green)
13. Buran TV Target
14. Laser Retroreflector No. 1
15. Flashing Light (White)
16. Laser Retroreflector No. 4
17. Centerline Shuttle Target
18. Approach / Rendezvous (Igla) Antenna
19. Deflection Plates
20. Mooring and Stabilization Engines
21. “Kurs” Docking System Parabolic Antenna

This is the docking port which will be used on STS-71 to connect to the Mir Complex. Discrepancies between this photograph and available diagrams of the docking unit are described in section 2.2.

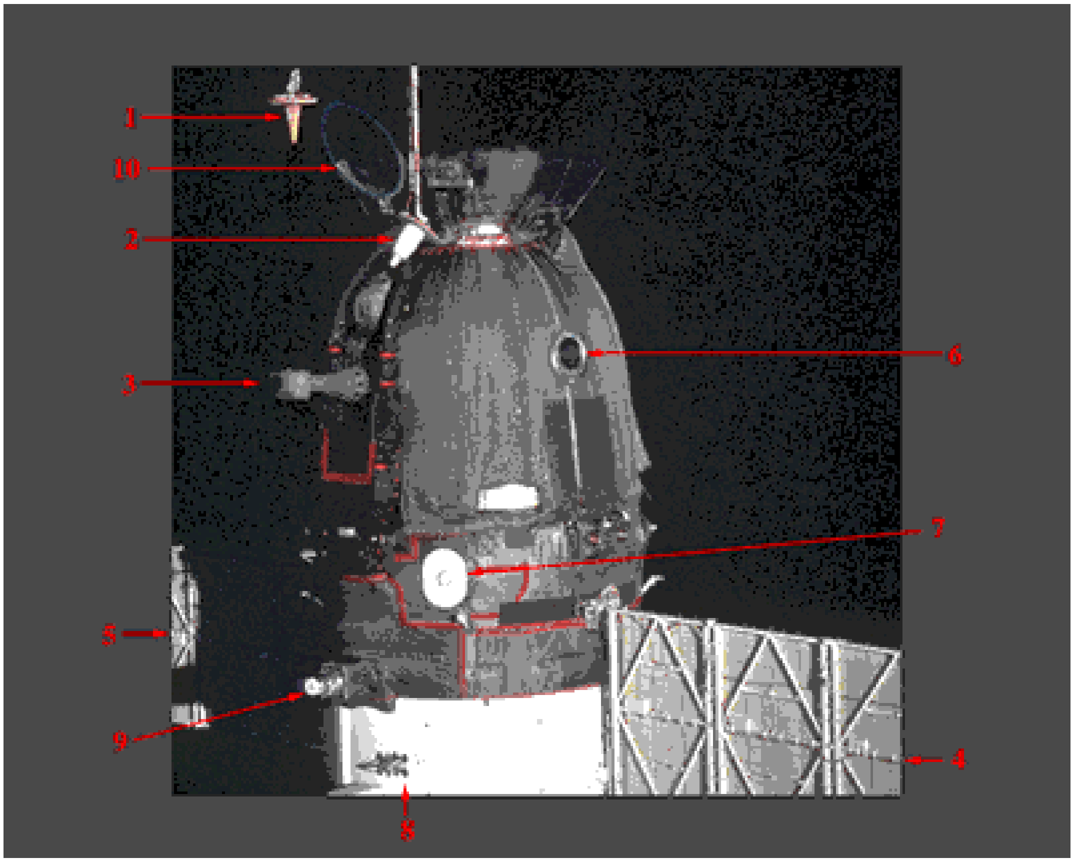

Figure 2-G Soyuz TM Capsule / Mir Module

1. Antenna
2. Approach and Rendezvous (Igla) Antenna
3. Instrument for visual orientation on the Earth and docking
4. Soyuz TM Port Solar Array
5. Soyuz TM Starboard Solar Array
6. Window
7. Command Radiolink Antenna
8. Antenna
9. Horizon Sensor
10. Landing Hatch Cover

Although the interface is not visible, Soyuz TM is connected to the end port of the Mir Base Block.

2.2 Configuration Documentation Discrepancies

Discrepancies between the expected and actual configuration of the Mir station are documented in this section.

In NASA Document # WG-3/NPO E/NASA/002/3402 0 the configuration of the Mir Complex has the locations of the Progress M and Soyuz TM spacecraft reversed.

Photography of the Kristall Docking Mechanism (see Figure 2-F) shows four connectors visible around the circumference of the docking frame. Both the diagram in NASA Document # WG-3/NPO E/NASA/002/3402 0 and the NASA Document "A Russian Space Station: The Mir Complex", show eight connectors around the circumference of the docking frame. The latter describes the connectors as: Fluid Connector Socket (2), Electrical Connector Plug (2), Electrical Connector Socket (2), and Fluid Connector Plug (2). Discussions with the Payload Integration and Engineering Office (MS2) indicate that this is not an issue for the STS-71 docking.

3. MIR SURFACE ASSESSMENT

A survey of the visible Mir station components was performed to identify areas of damage and discoloration. Measurements of this damage were obtained where possible. A complete tabular list of damage and discoloration (and the roll and frame numbers on which they were identified) is located in Appendix A.

3.1 Base Block

The Mir Base Block has been in orbit for more than nine years (three years beyond its anticipated life time). Light brown discoloration can clearly be seen on the module surface. This discoloration covers approximately 50% of the visible propulsion section surface. Also, the port window on the lower section of the Base block (near the bottom of the image) appears to slightly discolored.

A view of the non-pressurized assembly section (also known as the propulsion section) of the Mir Base block is shown in Figure 3-A. Area [1] shows the Igla antenna and Area [2] encompasses one of the meteoroid impact sensor panels.

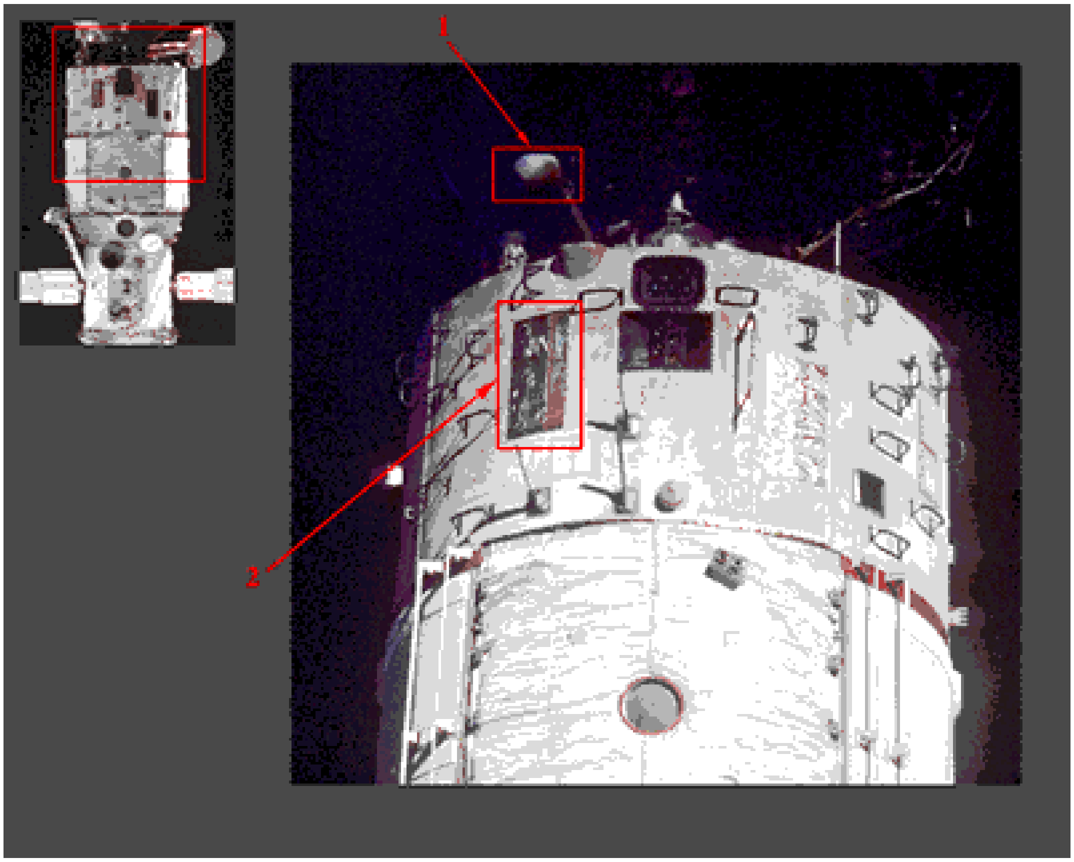

Figure 3-A Mir Base Block

Area [1] reveals the prominent dark brown discoloration seen on the Igla antenna. One possible reason for this discoloration could be deposition of particles (hydrogen, carbon dioxide, air and other micro contaminants) expelled from three drainage holes located just above the field-of-view on the forward section of the Kvant module.

Area [2] shows the damage on the meteoroid impact sensor surface material. Although two sensors are visible in this view, damage is only apparent on one. Three 95 cm by 15 cm strips appear to make up this panel. One of these strips appears to be missing. Additionally, a circular area with a 30 cm diameter appears to have surface material peeled off.

A view of the surface of the Mir Base block working compartment is shown in Figure 3-B. Area [1] includes the sunshade on the port window. Area [2] shows the foil-like material on the observation port window cover.

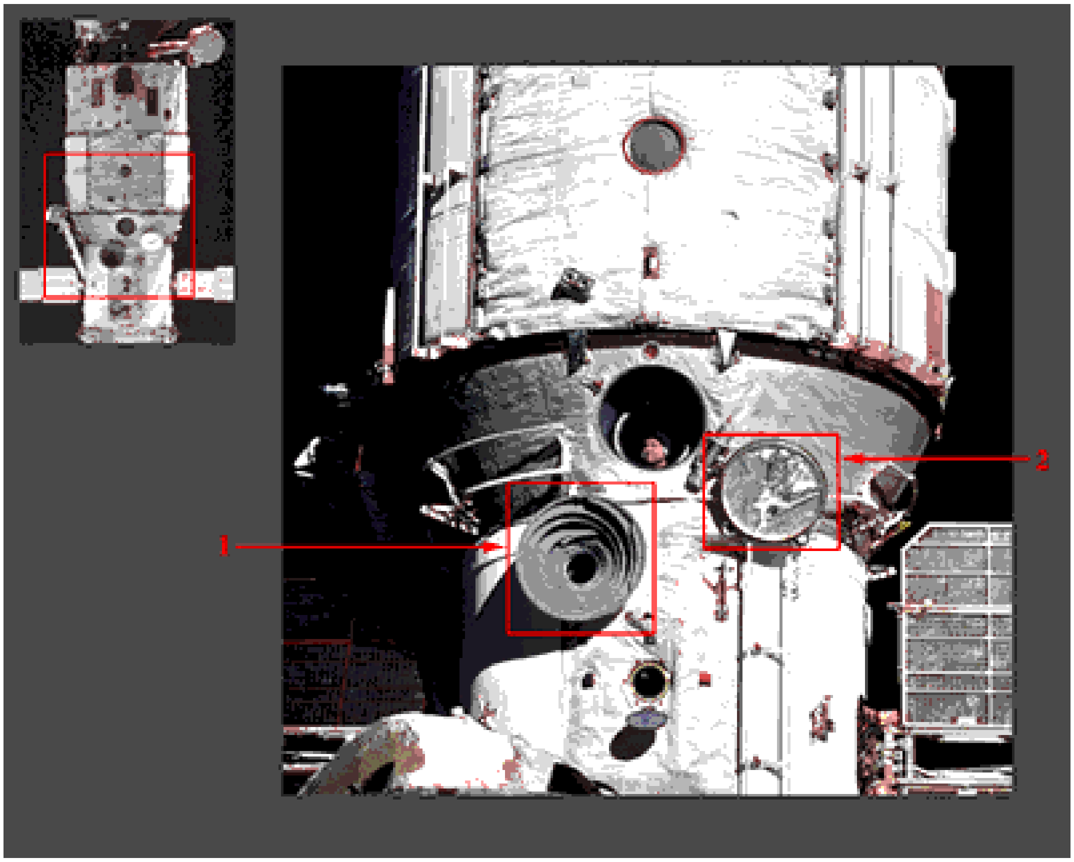

Figure 3-B Mir Base Block Working Compartment

Area [1] : Four possible impact damage locations are seen on the gray sunshade. The dimensions of these range between 4 cm^2 and 9 cm^2 . Analysis of the intensity variation on these damaged areas indicates a coarser surface than the surrounding region and suggests that the damage is caused by external impacts.

Area [2]: The foil-like material on the observation port window cover appears to be torn. The length of this tear is nearly equal to the diameter (74 cm) of the cover. This foil cover was seen to oscillate during the Shuttle's approach and backaway sequence. This event is documented in Section 5.

3.2 Kvant Module

A view of the Kvant module docked is shown in Figure 3-C. The two regions in Area [1] show the color variation on four surface panels. The regions in Area [2] show discoloration that may be due to external impacts on the surface.

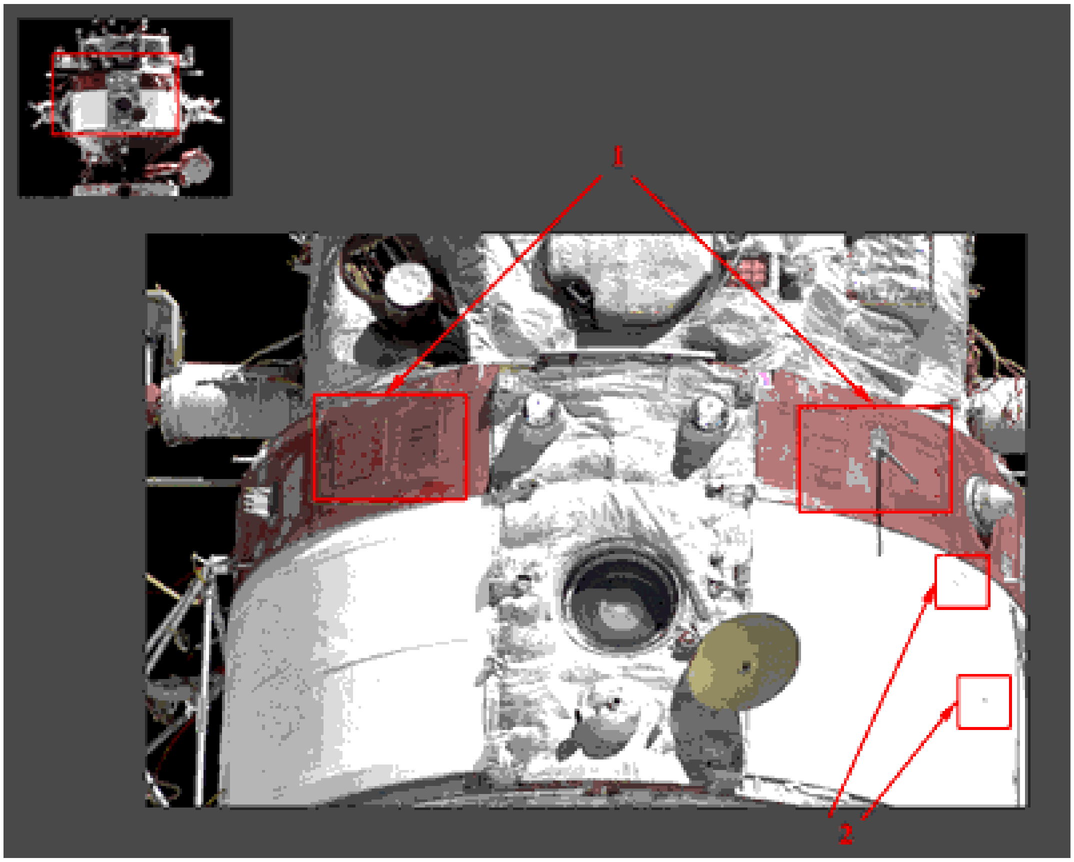

Figure 3-C Kvant Module

Area [1]: On the Kvant module, four attached patches of varying color shades are visible. The patches reveal color differences between the two areas that are not attributable to lighting differences.

Area [2]: Two different dark spots were identified on the work section module, probably due to external impacts. The larger impact location area is about 64 cm^2 in size while the smaller one is less than 4 cm^2 in size. Light intensity variations imply the discolored regions have a coarser surface than the surrounding area.

A detailed view of the forward section of the Kvant module docked with the Mir Base Block is shown in Figure 3-D. Area [1] shows the thermal protection blanket around the Kvant's conical shaped forward end beneath the mating system. Area [2] shows dark spots on the Mir Base Block's Luch antenna.

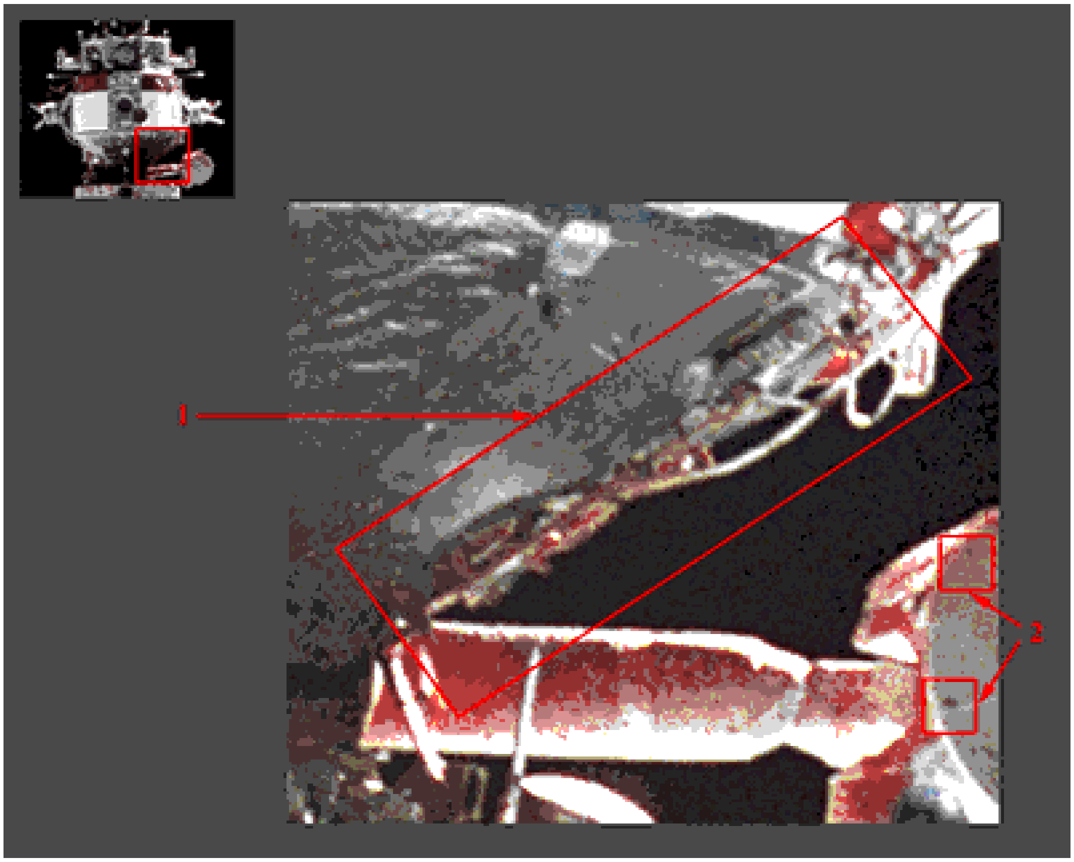

Figure 3-D Kvant Module Forward Conical Section

Area [1]: One end of the thermal protection blanket appears to be loose around the forward end of the Kvant module. [A more detailed view of this damage location can be seen on 35 mm film, roll 54, frame 22.] When the Kvant module was originally docked to the Mir station (in March of 1987), a foreign object was jammed in the docking unit and hampered the hard docking of the Kvant module to the Mir Base Block. An Extra Vehicular Activity (EVA) of more than 3.5 hours was required to dislodge the object. The physical nature of the EVA operation may have resulted in the thermal blanket damage on the Kvant module.

Area [2]: Dark spots were observed on the Luch antenna dish and supporting truss. The discoloration pattern may have resulted from sprayed contaminants. One possible source could be the eject holes in the forward section of the Kvant module designed to purge hydrogen, carbon dioxide, and air. The dimensions of the dark spots seen on the Luch antenna range between 9 cm^2 and 16 cm^2 .

3.3 Kristall Module Docking Mechanism

A view centered on the docking mechanism on the Kristall module is shown in Figure 3-E. This assembly is also known as the Androgynous Peripheral Assembly System (APAS) or Androgynous Peripheral Docking Unit (APDU). Area [1] highlights the Igla antenna system, Area [2] shows the Buran TV target, Area [3] encompasses discoloration on the thermal protection blanket and Area [4] reveals discoloration on the back plate of the attitude thruster engines.

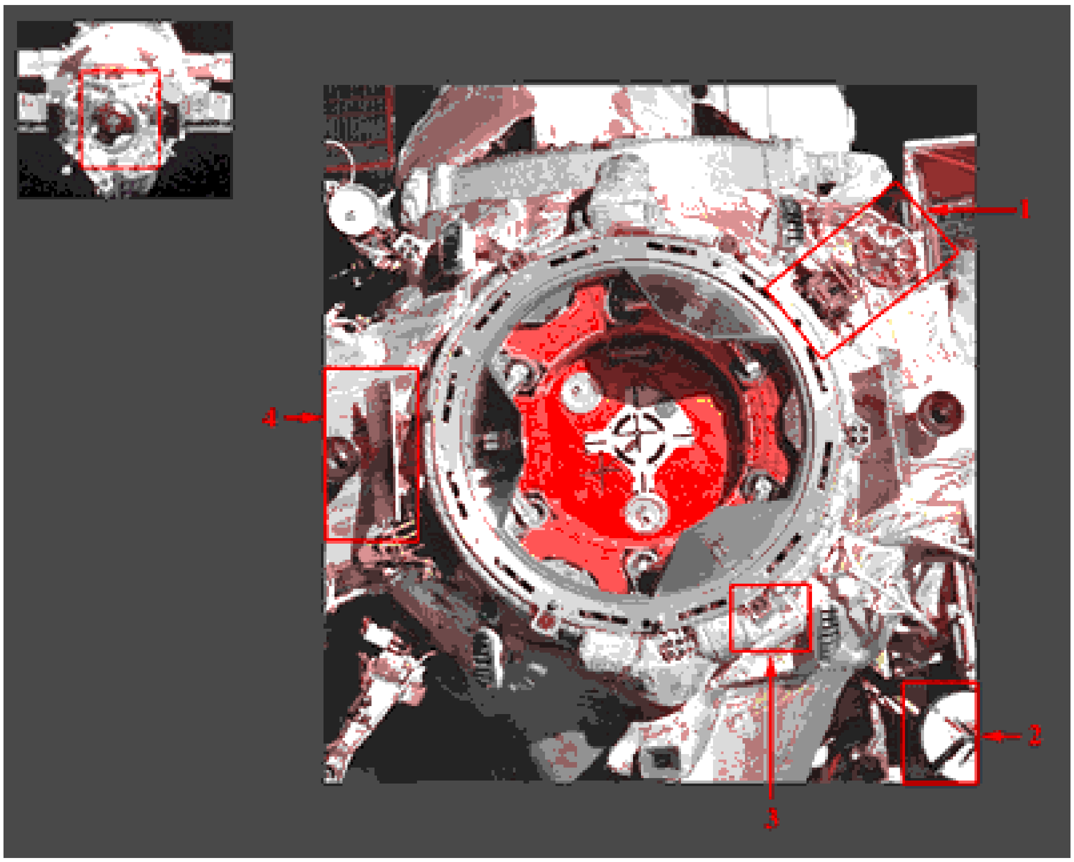

Figure 3-E Kristall Module APDU - Centerline

Area [1]: The Igla antenna system on the docking module is pointed toward the Kristall solar arrays. The antenna is probably not in an active mode in this orientation.

Area [2]: The surface of the Soyuz-TM target shows brown discoloration and several dark spots. These may have occurred on previous docking procedures.

Area [3]: The thermal protection system around the docking module has several folds and edges. Most of these edges show prominent discoloration. One such discoloration around the electrical / water connector on the docking module is shown as an example.

Area [4]: Prominent discoloration on the protective plate near the attitude control engines can be seen.

An off-center view of the Kristall module docking assembly and surrounding elements is shown in Figure 3-F. Area [1] includes the mooring and stabilization engines along with the back plate. Area [2] shows the standoff docking target. Area [3] indicates the uneven folds of the thermal blanket. Area [4] is the Soyuz-TM target.

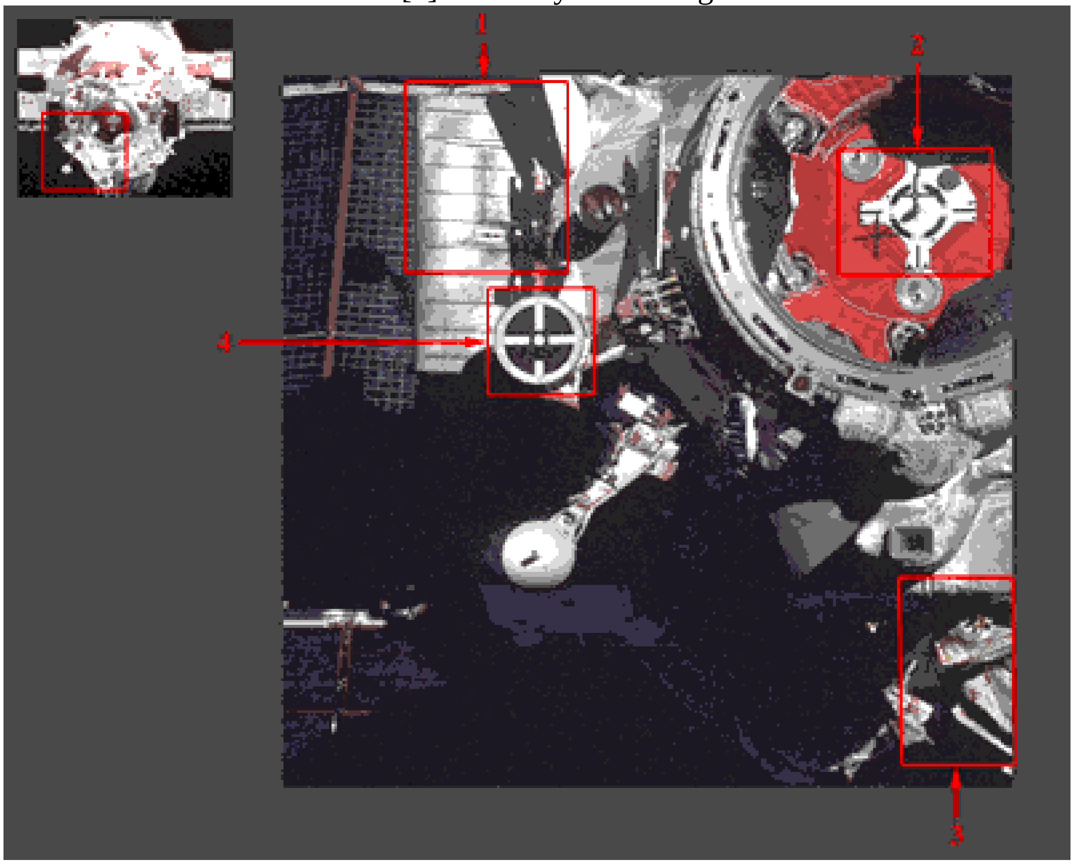

Figure 3-F Kristall Module APDU - Off-center

Area [1]: The mooring and stabilization engines may have caused the discoloration on the engine jackets as well as the back plate beneath the engines. The discoloration on the outer edges of the back plate also suggests that engine thrust contaminants go beyond the edges. This implies the possibility that damage could occur to the Kristall solar array panels from these thruster firings.

Area [2]: The back plate of the docking target shows some light yellow discoloration. The presence of this discoloration is apparent on the 70 mm film. However, the effect is not visible in the 35 mm image data. The apparent discoloration may simply be a reflection of the yellow cloth material in the background.

Area [3]: This area illustrates the uneven folds in the thermal protection blanket. Apparent discoloration of the blanket is also visible in this image.

Area [4]: The Buran TV target has several dark spots and brown discolorations.

3.4 Soyuz-TM Capsule

The descent module of the Soyuz-TM spacecraft is shown in Figure 3-G. Area [1] indicates possible impacts on the thermal blanket. Area [2] indicates a loose flap on the thermal blanket.

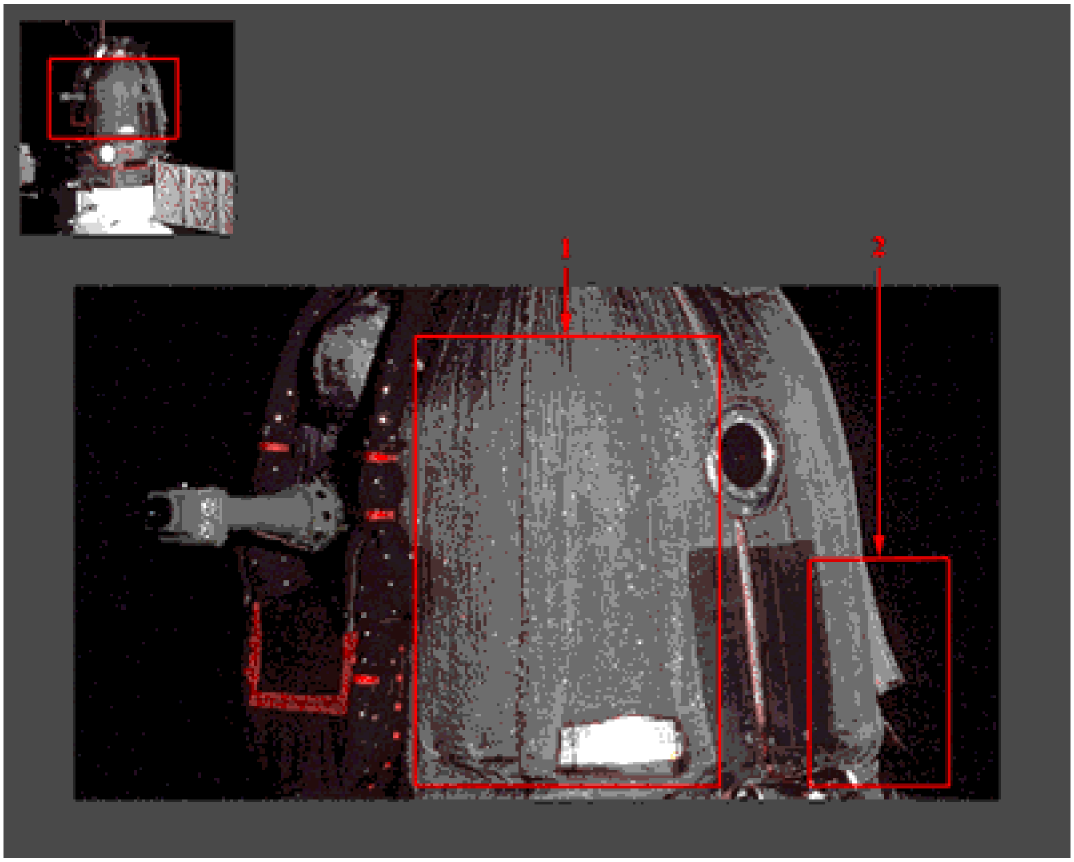

Figure 3-G Soyuz-TM Descent Module

Area [1]: Several small light discolored areas are seen on the thermal blanket of the Soyuz-TM descent module. This type of damage on the thermal blanket could be due to external impacts.

Area [2]: A loose thermal blanket is visible on the Soyuz-TM capsule. While this tear does not appear to be significant (~12 cm offset from the surface), severely damaged insulation could cause condensation during temperature extremes that occur during orbit. Soyuz-TM 9 (launched in February, 1990) experienced a more severe loss of thermal protection. Cosmonauts en-route to the Mir complex noticed that three of the eight thermal blankets came loose. These blankets were finally repaired through an extensive EVA after docking. Prior to the repair, the orientation of the entire Mir complex had to constantly be altered to maintain the proper temperature gradient for the Soyuz-TM capsule.

3.5 Solar Arrays

A port side (as viewed from the Shuttle during approach) solar array panel of the Mir Base Block is shown in Figure 3-H. Substantial damage is apparent in Area [1].

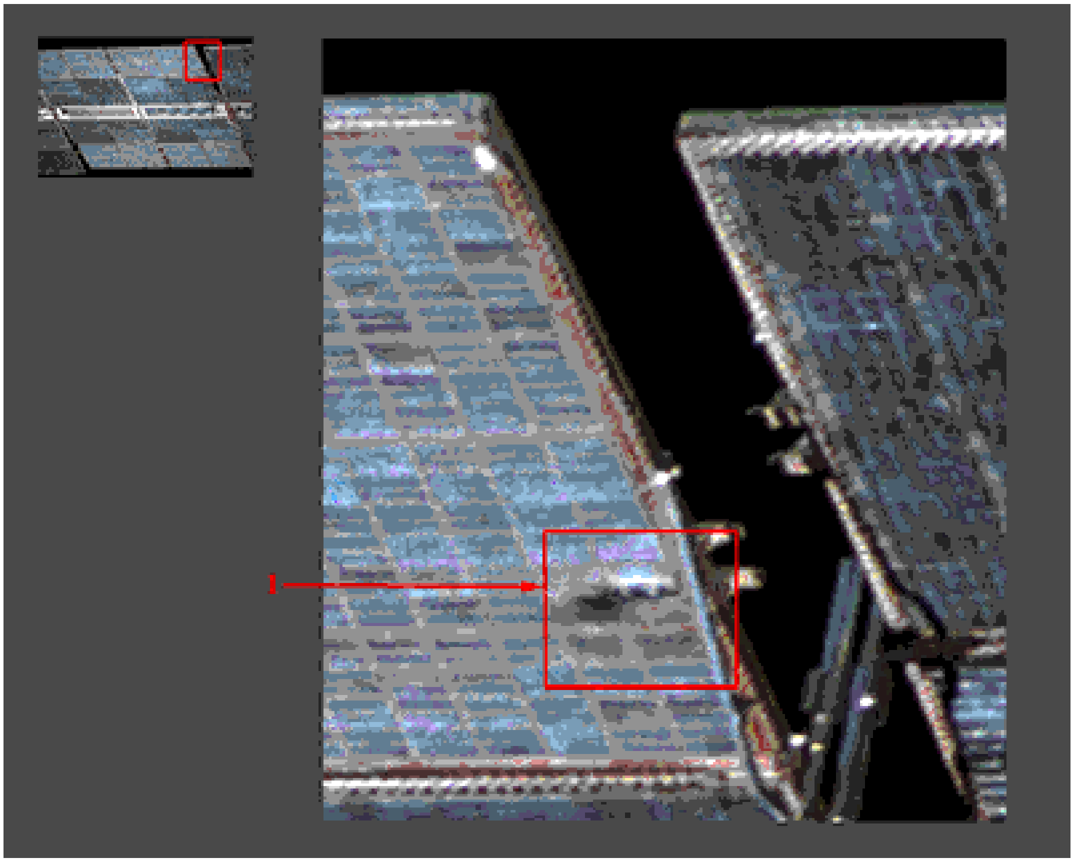

Figure 3-H Solar Array off Mir Base Block

Area [1]: The damage in Area [1] illustrates the possibility of an orbital debris strike where an object has apparently traveled completely through a panel. This area of damage encompassed a $27\ cm^2$ area. At least six adjacent cells appear to have suffered ancillary damage. Further analysis of this particular panel indicates slight warping within the frame structure.

Several cells on both panels of the Kristall module appear to be cracked or discolored. Possible reasons for such damage include: constant shade, attitude control engine thruster firings, electrical shorts and orbital debris impacts.

A port side (as viewed from the Shuttle during approach) solar array panel of the Kristall module is shown in Figure 3-I. Apparent damage can be seen on the panel in Area [1].

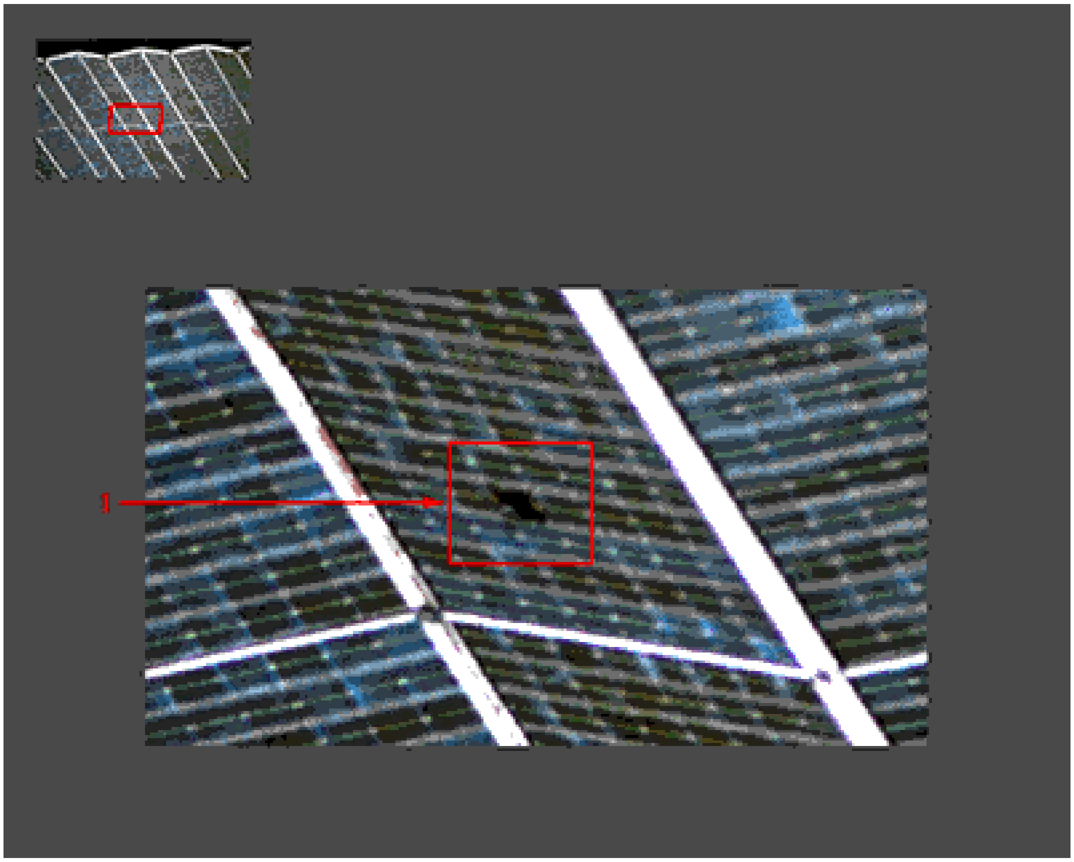

Figure 3-I Port Solar Array off Kristall Module

Area [1]: This top side view of the Kristall solar array reveals damage to one of the panels. Two or three individual solar cells are damaged or missing at this location. This could have been due to an external impact or electrical damage. The damage is approximately between $4\ cm^2$ and $16\ cm^2$ per side. The gray scale intensity variations of the damaged area do not correlate with that of the background. This implies that the hole does not go cleanly through the panel.

Several other areas of damage can be identified on the Kristall solar panels. A starboard side (as viewed from the Shuttle during approach) solar array panel of the Kristall module is shown in Figure 3-J. Apparent damage can be seen on the panel in Areas [1] and [2].

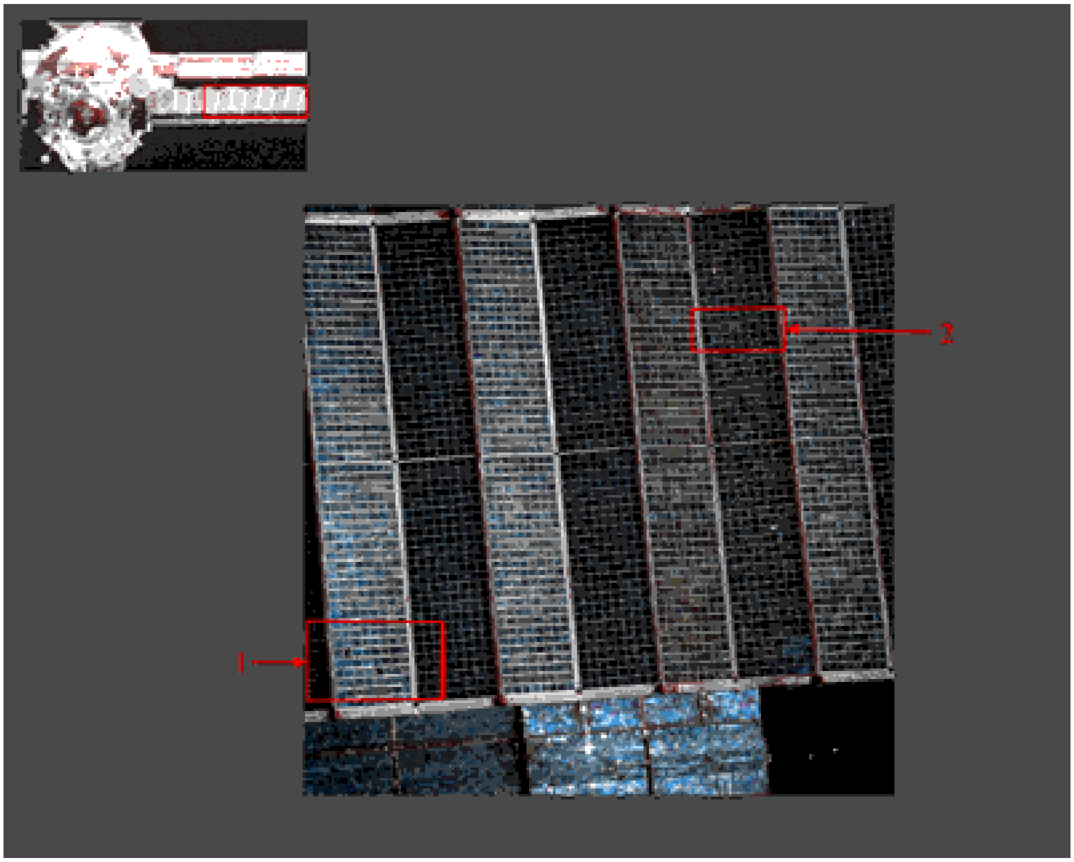

Figure 3-J Starboard Solar Array off Kristall Module

Area [1]: This top side view of the Kristall solar array reveals damage to two cells at the bottom left corner of the image. Two individual solar cells are damaged at this location. The damage was measured to be $25\ cm^2$.

Area [2]: This view reveals further damage to another solar cell located at the top right corner of the image. The damage size was measured to be about $25\ cm^2$.

More detailed damage assessment is documented in Appendix A.

4. TARGET VIEWING ASSESSMENT

A target viewing assessment was performed to evaluate the performance of the primary video cameras used during the rendezvous. This involved a comparison between Payload Bay Camera ‘D’ with a Monochrome Lens Assembly (MLA), the Color Television Camera (CTVC) located in the port window of Spacehab, and the handheld camcorder. This imagery is referenced to the best still photography acquired from the Hasselblad 70 mm film camera.

4.1 Target Acquisition Times

Crew members have stated that target features were visible to the eye well before any of the video cameras were able to resolve them. The table below documents a comparison of the acquisition times of the docking mechanism and standoff docking target. Camcorder data did not have timing and imagery of the target was sporadic. The still photography timeline could not be accurately quantified since pictures of the target were not taken continuously.

camera	docking mechanism features	standoff docking target
PLB ‘D’ - MLA	19:15:22	19:24:12
Centerline - CTVC	19:14:31	19:25:24

Table 4-A Target Acquisition Times

4.2 Target Visibility Comparison

Hasselblad (70 mm) photography provided the best views of the APDU. The docking structural latches, capture latches, body-mounted latches, alignment guides, laser retroreflectors, fluid/electrical socket/plug, and the centerline target all appeared to be in good condition. Some minor discoloration to the backing material was noted and is documented in Section 3.3.

Figure 4-A documents views of the target from the MLA, the CTVC and the handheld camcorder. All pictures were taken at about the time of closest approach. However, lens and aperture or iris settings varied greatly. Therefore, direct comparisons of the different views are not possible.

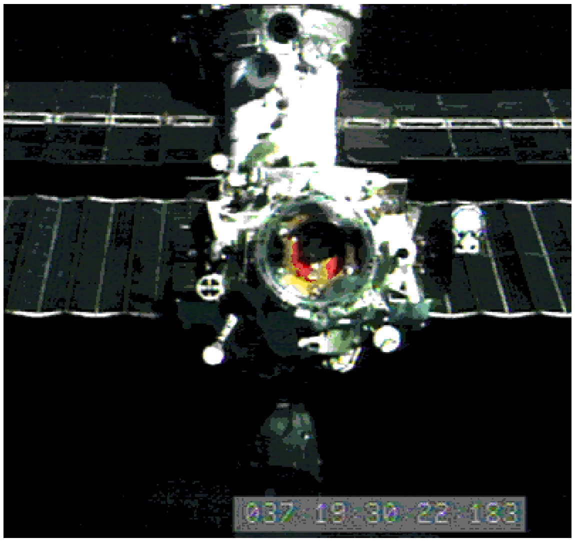

CTVC

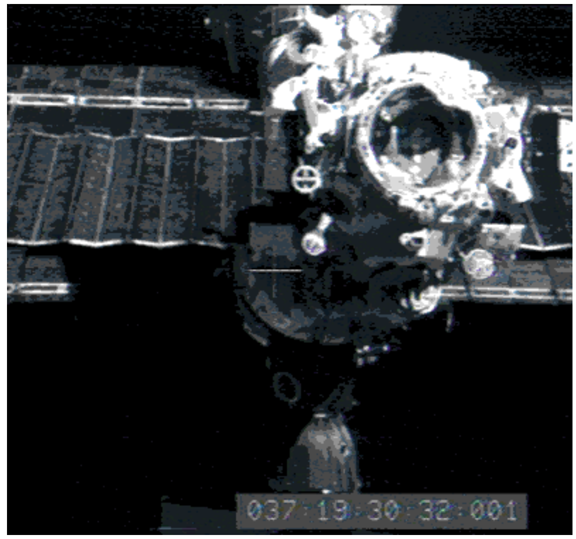

MLA

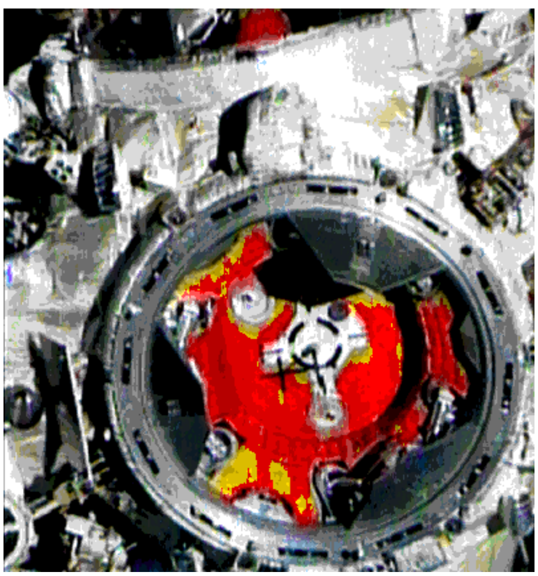

CMC

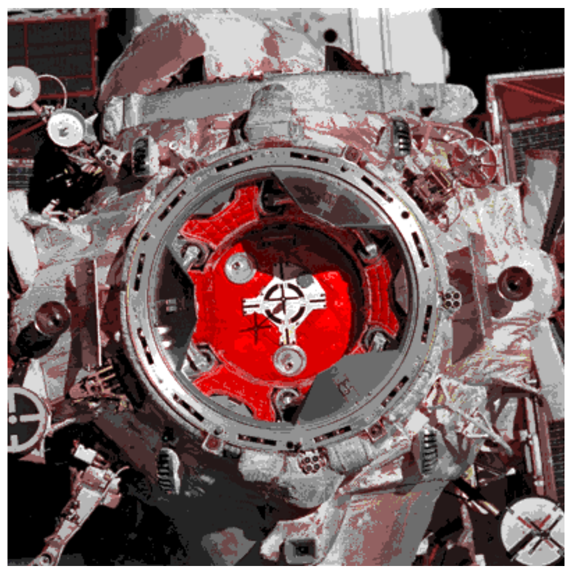

70 mm

Figure 4-A Target Visibility Comparison

The 70 mm photograph shows a level of detail presently only possible on film. The MLA and CTVC images did not reveal much detail inside the docking mechanism, especially where the target was in shadow. However, since their iris and zoom settings were not adjusted to maximize dynamic range and resolution characteristics, a fair evaluation of these two cameras can not be performed. The camcorder's ability to extract information even when the target is in shadow may be useful for viewing events which occur in low light level conditions.

5. PLUME IMPINGEMENT

5.1 Impingement Data

The original plan on obtaining data for the plume impingement analysis was limited to video gathered during the initial backaway sequence. This procedure involved setting up PLB cameras 'A' and 'B' to point at one of the Core module array tips in a muxed mode (where only the center half of each image is captured on one view). The reasons for using a dual camera setup were two-fold: the CTVC camera in position 'B' resolved motion well and the WLA in position 'A' would see better in low light level conditions (which at the time of the flight plan was not definite), and if such motion was significant enough to measure, these views would allow for a stereoscopic phototheodolite analysis. Due to crew time constraints during the station-keep phase at closest approach, however, the planned views were not set up until several minutes after the backaway began. At that time, no movement of the solar array tips could be discerned.

5.2 Correlation with Shuttle RCS Thruster Firings

Video imagery of the Mir station during the rendezvous did reveal an alternate source for detecting plume impingement. A torn foil cover on one of the Mir Core ports (see Figure 3-B) appeared to oscillate at different times during the approach and backaway. Observances of this motion were correlated with Shuttle RCS thruster firing data during the approach and backaway. A strong correlation was found to exist between the foil cover oscillation and the firings of the F2F and F3F thrusters. No measurements could be gleaned from this analysis, however, since both the material type and the exact nature of the tear could not be identified.

The presence of an apparent offset between the video data and the thruster firing data is being investigated. Resolution of this issue will enable a statistics-based correlation analysis of these two sets of data.

6. MOTION ANALYSIS FROM FILM AND VIDEO

A test was performed to evaluate the accuracy of photographic and video data in calculating distance from the Shuttle to the Mir as a function of time. Trajectory Control System (TCS) data available during the rendezvous has errors on the order of approximately +/- 2 feet. Analysis using standard Orbiter photographic and video equipment should prove to be useful to identify error sources on future missions when more accurate devices are not necessarily available.

Video and still photography coverage of the Mir from the Shuttle during approach, fly-around and backaway was reviewed. The video coverage, obtained from the CTVC centerline camera, was used to assess lighting conditions during these times since parts of the rendezvous occurred during darkness. Measurements were made from both video and still footage to determine the relative motion between the Shuttle and Mir during approach, fly-around, and backaway. Still photography data was collected from both 35 mm and 70 mm film. However, uncertainties about the lenses used during the approach and backaway procedures precluded the use of still photography in this comparison. However, the video measurements were compared with those taken using the TCS. A diagram showing the locations of the cameras used in the Mir survey is presented in Appendix D.

Figure 6-A compares actual TCS data with that from the CTVC centerline video camera. The CTVC camera distance calculations utilized horizontal-field-of-view information embedded in the vertical interval.

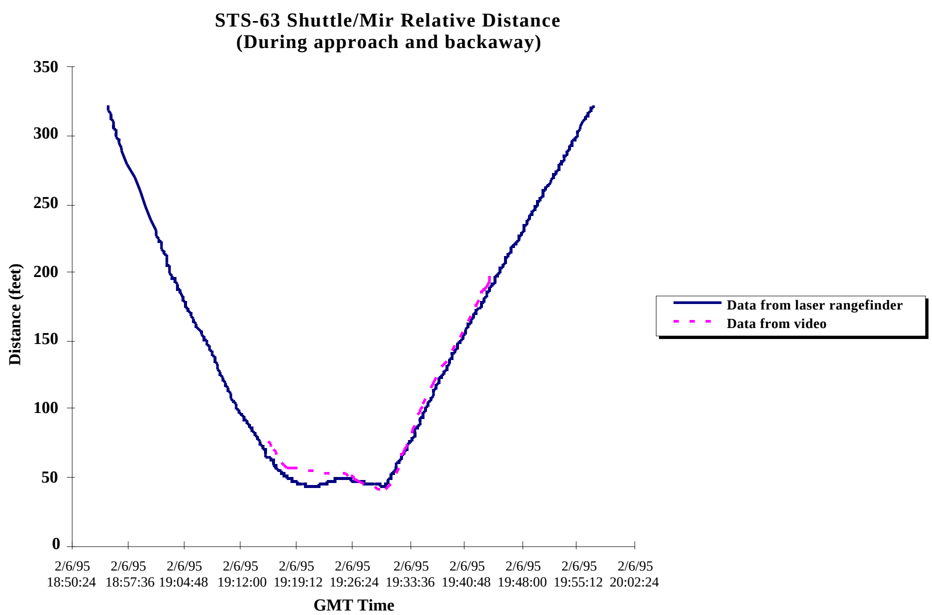

Figure 6-A Shuttle/Mir Relative Distance During Approach and Backaway

This chart shows that distance calculations based on CTVC camera data appeared to be consistent with the more accurate TCS data during the daylight portions of approach and backaway. However, no information could be gathered from these views during darkness. Fly-around data did not show sufficient detail to extract accurate scaling information.

7. ANTENNA TRACKING

The Luch satellite communications antenna on the Core module was seen in different orientations during the rendezvous. This raised the concern of possible occurrences where the Shuttle Ku-band antenna could be looking directly at the Mir antenna. In the event of such an occurrence where both antennae were active, damage to their corresponding communication systems could have resulted. Radiation resulting from antenna cone angles intersecting the Shuttle could also be a crew safety issue. Two types of motion were visible: that of the antenna arm, and of the dish itself.

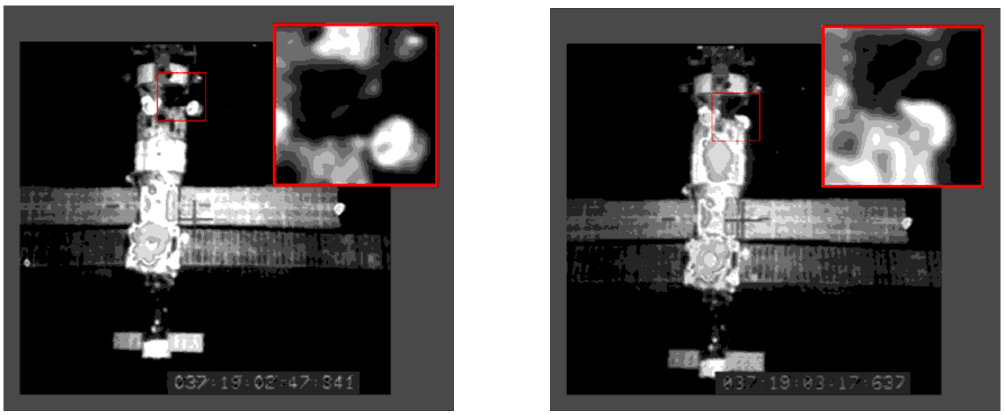

Figure 7-A Luch Antenna Arm Orientation

The CTVC centerline camera could not image the Luch antenna arm while it was in motion during the approach. The MLA camera at the PLB 'D' position tracks the arm motion during this time. (See Figure 7-A.) The Luch antenna arm starts to rotate at approximately 37:19:02:48 GMT and stops at approximately 37:19:05:02 GMT. The antenna is initially oriented at 36° about the Mir X-axis and 22° about the Z-axis (pointing above and toward the starboard side of the Orbiter.) The angular motion of the antenna arm is about the Mir's X-axis with the dish turning away from the Space Shuttle. The rotation rate of the antenna arm was measured to be 35°/minute.

The Luch antenna arm is also in motion during the fly-around as seen on PLB camera 'D'. The time interval for this motion is 37:20:40:37 GMT to 37:20:41:26 GMT. Since the Mir and Orbiter are both changing attitudes, no accurate measure of antenna orientation could be calculated.

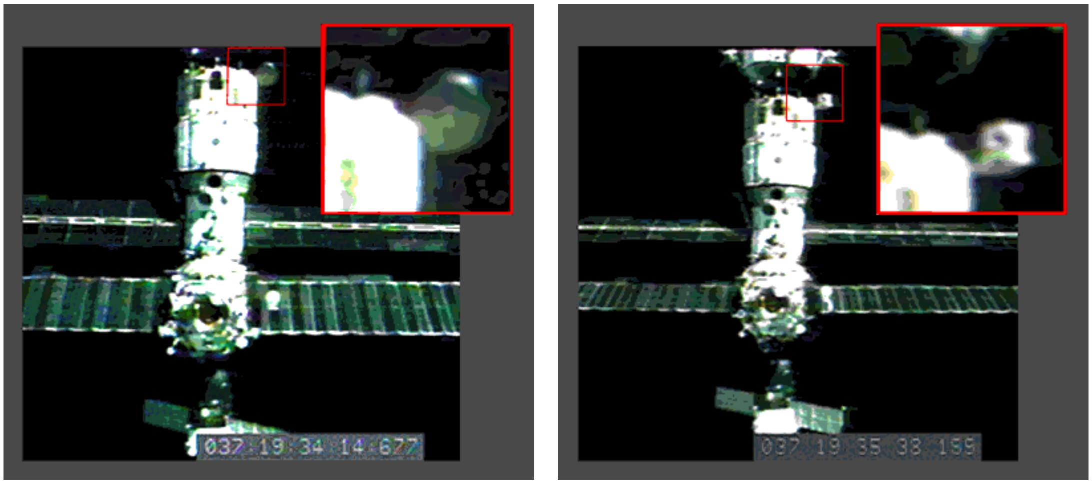

Figure 7-B Luch Antenna Dish Orientation

The Luch antenna dish first enters the CTVC centerline camera's field-of-view at 037:19:34:01 GMT. This time is during the early part of backaway when the Orbiter is about 80 feet away from the Mir Station. (See Figure 7-B.) Initially, the dish is oriented at 9° about the Mir X-axis and 18° about the Z-axis (pointed in the general direction toward, but below and off to the port side of the Orbiter.) The dish starts to rotate at 37:19:34:10 GMT and stops at 37:19:35:23 GMT. The antenna dish rotates 10° about the Mir X-axis and 60° about the Z-axis (with the antenna's orientation approximately parallel to the Mir's Y-Z plane.) The rotation rate of the antenna dish was measured at 53° /minute.

A second movement of the antenna dish was noted between 037:19:42:02 GMT and 037:19:43:32 GMT. The antenna dish rotated back, again pointing in the general direction of the centerline camera.

In conclusion, although the Luch antenna was never seen pointing directly at the Orbiter, it appears that the antenna was pointing in the general direction of the Shuttle at least during several minutes of the backaway. Due to measurement errors in determining antenna orientation in 3 dimensions, errors are estimated to be in the range of +/- 5°. Actual antenna cone angles and activation times would be required to perform further analysis from the available data.

8. SOLAR ARRAY SUB-PANEL DEFLECTION

Small offsets between sub-arrays were noted on some of the Mir solar panels. These deflections might have an impact on loads analysis when the Shuttle and Mir are in a docked configuration. Offset angles between consecutive sub-panels on the Core and Kvant-2 modules were measured from selected 70 mm film views. The diameter of the Mir Core module was used as a scale factor for all measurements.

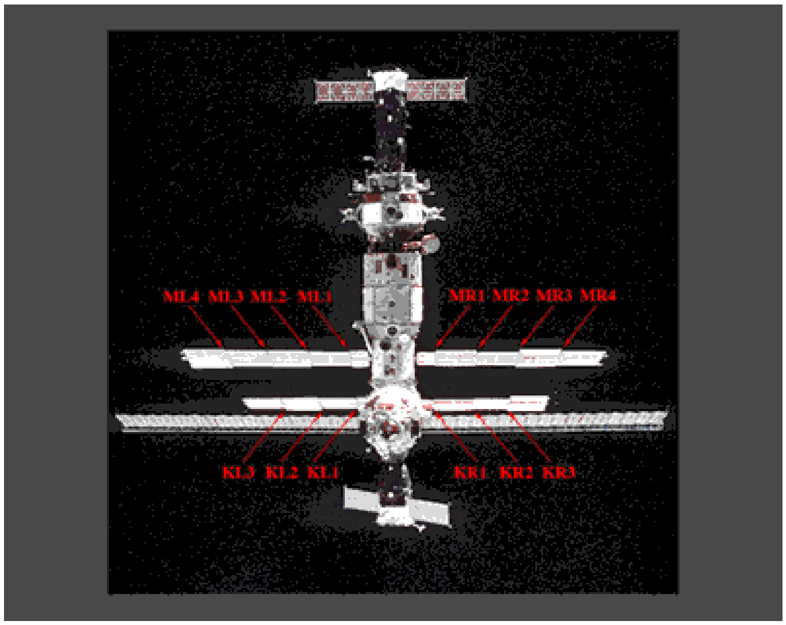

Figure 8-A Solar Array Sub-panel Nomenclature

Figure 8-A shows the different offset angles that were measured. The panels were assumed to have no bends in their structural supports. Sub-array panel offset angles are shown in the accompanying table:

	ML4	ML3	ML2	ML1	MR1	MR2	MR3	MR4
Mir	2.7°	2.9°	3.1°	3.1°	3.1°	3.1°	2.9°	3.2°
		KL3	KL2	KL1	KR1	KR2	KR3	
Kvant-2		3.9°	2.3°	2.3°	n/a	4.6°	3.6°	

Table 8-A Solar Array Offset Angles

n/a - can not be determined due to the bending of the sub-array panel.
Note: Measurement errors correspond to approximately +/- 1° in the offset angle.

9. PRODUCT EVALUATION

This section discusses overall quality of the film and video data. Scenelists with more detailed information about individual films and videos are included in Appendices B and C. The pre-mission data acquisition timeline is presented in Appendix E.

9.1 Film Summary

In general, still photography provided only adequate imagery of the station configuration. Notable exceptions to this were detailed imagery of the docking mechanism and the Mir Base block. While more photography was acquired with the Nikon than the Hasselblad, there appeared to be more problems with the 35 mm data (Nikon). Table 9-A provides information about data acquisition times for the different films.

Roll #	*camera*	*# frames*	*far approach*	*approach*	*station-keep*	*backaway*	*fly-around*	*separation*
708	70 mm	77				**x**	**x**	
710	70 mm	8	**n/a**	**n/a**	**n/a**	**n/a**	**n/a**	**n/a**
711	70 mm	99	**n/a**	**n/a**	**n/a**	**n/a**	**n/a**	**n/a**
712	70 mm	80	**n/a**	**n/a**	**n/a**	**n/a**	**n/a**	**n/a**
713	70 mm	89	**x**					
9	35 mm	31	**x**					
10	35 mm	37		**x**				
11	35 mm	37		**x**				
13	35 mm	29		**x**				
28	35 mm	15		**x**	**x**	**x**		
30	35 mm	37		**x**				
31	35 mm	37				**x**		
32	35 mm	37				**x**		
51	35 mm	37				**x**		
52	35 mm	28				**x**		
53	35 mm	34	**x**					
54	35 mm	37	**x**					
55	35 mm	37			**x**			
56	35 mm	38	**x**					
57	35 mm	37	**x**					
58	35 mm	35	**x**					
59	35 mm	37	**x**					
316	35 mm	37					**x**	
318	35 mm	37					**x**	**x**

Table 9-A Onboard Still Photography of Mir Rendezvous Events

9.1.1 35 mm Photography

The Nikon F4 camera was used to capture 654 frames of Mir photography. This photography covered all phases of the rendezvous. The most complete coverage occurred during the approach and backaway phases. All major components were visible on the 35 mm film. However, Kvant -2 was the only module that did not have adequate imagery for analysis. Mir configuration verification and damage assessment were the primary uses for the resulting views. Exposure time was recorded on all 35 mm rolls.

Imagery captured with the Nikon F4 had varying degrees of quality. The percentage of useful imagery captured on 35 mm film adequately complemented the total image acquisition for the DTO. Images which were not useful generally exhibited one or more of these characteristics: soft focus, inadequate exposure, shallow depth of field, or camera motion.

9.1.2 70 mm Photography

The Hasselblad camera was used to capture 353 frames of Mir photography. The timing on 3 of the 5 magazines malfunctioned and prohibited coordinating images to rendezvous phases. However, the imagery captured on these magazines were used as the primary media for most configuration and damage assessment analyses. As with the 35 mm photography, imagery of the Kvant-2 module was not successfully captured.

Imagery captured with the Hasselblad were general good in quality. This photography made up the majority of the useful still imagery for DTO-1118. Images which were not useful exhibited soft focus or shallow depth of field.

9.2 Video Summary

In general, payload bay camera views only provided overview imagery of the station configuration. Notable exceptions to this were detailed imagery of the docking mechanism and some of the solar panels. The effect of shadows on both the MLA and CTVC views of the Mir was to hide either the dark or lit regions completely. Most of the detail on component surfaces was captured on camcorder video. These views provided excellent coverage of the Kristall docking mechanism and its associated targets, most of the solar panels, and approximately half of the Core module and Progress and Soyuz capsules. Due to part of the fly-around occurring in the dark, detailed information of the Kvant-2 module was not acquired. Limited coverage of the Mir was obtained from a film-to-video conversion of onboard 16 mm film. Table 9-B provides information about data acquisition times for the different videos.

location	*camera / lens type*	*video ID #s*	*far approach*	*approach*	*station-keep*	*backaway*	*fly-around*	*separation*

centerline	CTVC	11, 13, 14, 16	x	x	x	x	x	x
PLB ‘A’	WLA	10, 13	x	x				
PLB ‘B’	CTVC	10, 18	x				x	x
PLB ‘C’	MLA	none						
PLB ‘D’	MLA	10, 13, 18	x	x	x	x	x	x
FAD o/h window	camcorder	39			x		x	

Table 9-B Onboard Video Coverage of Mir Rendezvous Events

9.2.1 Centerline (CTVC)

Approximately 4 hours of centerline CTVC camera footage of the rendezvous was captured. During the early portion of far approach, the image of the Mir appeared to be saturated. As the shuttle’s orbit entered darkness, the image of the station became sharper as the Orbiter moved closer. During the early part of approach, which occurred in darkness, only the Mir’s flashing lights were visible. At the time of closest approach when the docking mechanism was in shadow, crew members momentarily zoomed in on the target. During station-keep, at the time of closest approach, the image of the Mir appeared to be completely saturated for approximately four minutes. Most of the fly-around occurred in darkness where only the station lights were visible. The camera iris was opened for a few seconds to view Mir thruster firings as the station adjusted its orientation near the end of the fly-around.

During most of the rendezvous the camera’s focal length was set at 12.4 mm. The actual zoom range available to the CTVC camera is 5.5 mm to 47.0 mm. During daylight coverage, the picture appeared to be usable. However, the limits of resolvability could not be identified because the zoom was only changed once and was not accompanied by a change in the contrast to maximize visibility. In darkness, the only visible features on the Mir were the lights. Imagery of the docking mechanism and targets did not provide the level of clarity to do more than a cursory analysis.

9.2.2 Payload Bay Camera ‘A’

Less than 1 hour of PLB ‘A’ WLA camera footage of the rendezvous was captured. During the early portion of far approach, the image of the Mir appeared to be saturated. Approximately ten minutes of approach footage was obtained, mostly in darkness.

Camera ‘A’ was primarily used to view IMAX camera operations within the payload bay. The actual zoom range available to the WLA camera is 8.2 mm to 25 mm. Zoom ranges and resolvability issues could not be addressed from the available views. Imagery of the docking mechanism and targets did not provide the level of clarity to do analysis because the camera was not pointed at the Mir during the daylight phase of approach.

9.2.3 Payload Bay Camera ‘B’

Approximately 1.5 hours of PLB ‘B’ CTVC camera footage of the rendezvous was captured. During the early portion of far approach, the image of the Mir appeared to be saturated similar to the centerline CTVC camera. Approximately 15 minutes of fly-around and separation footage was obtained.

The camera ‘B’ CTVC was not used extensively during the rendezvous except for the far approach. As with the centerline CTVC camera, very little was done with varying zoom ranges and iris settings.

9.2.4 Payload Bay Camera ‘C’

No PLB ‘C’ video of the rendezvous was recorded onboard.

9.2.5 Payload Bay Camera ‘D’

Approximately 2 hours PLB ‘B’ camera footage of the rendezvous was captured. During the early portion of far approach, the image of the Mir appeared to be saturated. As the shuttle’s orbit entered into darkness, the image of the station became sharper as the Orbiter moved closer. During the early part of approach, which occurred in darkness, the lights on the Mir saturated most of the image. During station-keep, at the time of closest approach, the image of the Mir was saturated for approximately 5 minutes. In addition, the camera iris appeared to be opening and closing in an attempt to adjust to changing light conditions for approximately 30 seconds. During the early part of backaway, the camera field-of-view was changed to image the solar panels as part of the plume impingement task. Only a few minutes of the dark phase of the fly-around were captured and, once again, lights on the Mir saturated the image.

The actual zoom range available to the MLA camera is 18 mm to 108 mm. During daylight coverage, the picture appeared to be usable. However, limits of resolvability could not be identified because contrast adjustments to maximize visibility were not performed. In darkness, lights on the Mir tended to wash out most features. The MLA was to provide a backup view of the docking target if light levels were too low for the centerline CTVC. Utilization of camera settings as a function of lighting condition would have helped in the post-mission analysis.

9.2.6 Camcorder

Approximately 0.5 hours of camcorder footage of the Mir station was captured. The majority of this coverage occurred between approach and backaway along with a few minutes of the fly-around. Camcorder imagery appeared to be sharp and showed good dynamic range. During the few moments of approach when the camcorder was used while the orbit was in darkness, some detail of the docking area was visible. Imagery of the Mir acquired during station-keep provided the best downlinked views of the station.

No timing data was available for the camcorder views. Downlinked video from the camcorder provided the first detailed imagery of the surface condition of the Mir station. These views helped identify damage on the higher resolution still photography. Camcorder imagery provided the best video of the docking target during station-keep. Even when the Kristall APDS was partially in shadow, the camcorder was able to automatically adjust to the varying lighting conditions.

10. CONCLUSIONS AND RECOMMENDATIONS

10.1 Russian Review

RSC-Energia reviewed the contents of this report and issued the following conclusions:

Analysis of the photographs showed that after a 9.5 year term of operation, many materials of the exterior surfaces are in good condition (the optical coatings of the thermal control system radiators, the exterior layer of the vacuum shield thermal insulation). At the same time, a number of materials have suffered significant visible changes under exposure to space flight factors and contamination (for example, the exterior layers of the vacuum shield thermal insulation rods of the pencil beam antenna).

Experiments studying the external condition of the Mir station by taking still photos and video recordings are important for monitoring the materials of the station's exterior surfaces and in the future should be used to issue recommendations confirming its functionality and prolonging the station's service life.

10.2 Conclusions

10.2.1 Assessment of Procedures

Data gathered from the STS-63 rendezvous provides baseline imagery for comparison to subsequent docking missions. Several conclusions can be drawn from the procedures used to acquire film and video data:

- Still photography acquired of the docking mechanism area was excellent.
- Exposure and focus problems on the 35 mm film hampered analysis.
- 70 mm film provided the best still imagery of the rendezvous.
- Crew time constraints negatively impacted acquisition of plume impingement data.
- Payload bay video camera settings were not adjusted to maximize quality.
- Features in shadow could not be resolved on the payload bay camera videos.
- Camcorder video was not obtained systematically (random scene acquisition).
- Camcorder data provided the most detailed video imagery of the rendezvous.
- Payload bay lights appeared to be adequate for daylight data acquisition.
- Information embedded in the vertical interval of the CTVC video was useful for distance calculations.

10.2.2 Discussion of Results

The Mir Photo/TV survey performed on STS-63 provided useful information about the condition of the exterior surfaces of the Station. Twenty-five separate occurrences of damage and discoloration are documented in Appendix A. The discoloration seen on different Station components is probably a result of propellant residue from Mir RCS thrusters. Although no video was available of plume impingement upon the Mir solar arrays, correlation of the motion of a mylar cover on the Base Block to Shuttle RCS thruster firings indicated the presence of some plume impingement during the Orbiter's approach and backaway. Also, analysis of the orientation of the Mir's Luch communications antenna during the course of the rendezvous revealed instances where the antenna appeared to be pointing in the general direction of the Orbiter. This issue could be of concern on future missions if the Orbiter and Station communications antennae were pointing directly at each other while in an active mode.

10.3 Recommendations

STS-71 is scheduled to launch on June 24, 1995. Current plans call for an abbreviated fly-around. There are also tentative plans for Soyuz to separate from the Mir to view the undocking of the Orbiter. These changes have made crew time a premium on this mission. Therefore, DTO-1118 data acquisition procedures need to be streamlined. The following recommendations have been made:

- Change primary still camera from the Nikon (35 mm) to the Hasselblad (70 mm).
- Include diagrams in the Flight Data File to assist crew members identify image targets during the rendezvous.
- Highest priority remains obtaining still photography of the docking mechanism both prior to docking and after undocking.
- Emphasize systematic data acquisition procedures for still photography and video during crew training.
- Utilize ground control of payload bay video cameras to perform Mir surveys during crew sleep periods.
- Require seven daylight passes (assuming 1 crew member) to collect the desired information for the survey.

10.4 Other Issues

Lighting tests performed by the Flight Design and Dynamics Division (DM34) and the Flight Crew Support Division (SP3) indicated that shadows could affect visibility of the target during the STS-71 approach. Crew members will utilize the high intensity search light to view the target if the docking mechanism is in shadow.

Subsequent rendezvous missions are expected to generate at least as much data for DTO-1118 as STS-63. This information will need to be cataloged and indexed as the extent and scope of imagery increase. IS & AG will develop and maintain a relational database that catalogs images documenting rendezvous events. Inputs from multiple missions can be incorporated into long-term analyses to study degradation of different surfaces or to monitor configuration changes. The data will be required to be in a form which will allow users of the imagery to perform searches on Mir components including: clarity of image, location and type of camera, event time (in GMT), type of damage and related analysis.

11. APPENDICES

Appendix A	**STS-63 Mir Surface Damage / Discoloration**
Appendix B	**STS-63 Film Scenelist**
Appendix C	**STS-63 Video Scenelist**
Appendix D	**STS-63 Camera Layout**
Appendix E	**STS-63 Data Acquisition Timeline**

Appendix A

STS-63 Mir Surface Damage / Discoloration

Appendix B

STS-63 Film Scenelist

Appendix C

STS-63 Video Scenelist

Appendix D

STS-63 Camera Layout

Appendix E

STS-63 Data Acquisition Timeline

Appendix E

STS-71 Camera Layout

Appendix F

STS-71 Data Acquisition Timeline